

Methods

Genetic mapping and positional cloning

Heterozygous female fish (AB/EK) carrying the *foggy* mutation were crossed with wild-type male fish from a Tu genetic background. F₂ progeny were identified and separated into wild-type, heterozygous and mutant pools of 40 individuals. DNA from these fish was used for AFLP analysis (see Supplementary Information). We used polymerase chain reaction (PCR) primers corresponding to the two most closely linked AFLP markers to screen BAC (Genome Systems) and yeast artificial chromosome (Research Genetics) libraries and to initiate chromosomal walk. Individual BACs were then injected at a concentration of 40–60 ng μl⁻¹ into 1–2-cell stage zebrafish embryos derived from *foggy* heterozygous mating. BAC B108J11, which rescued the *foggy* mutant phenotype, was digested with *Eco*R1, random-primed with p32, and used to screen a 33-h embryonic zebrafish cDNA library. Full-length cDNAs were cloned into the vector containing β-actin promoter, injected at a concentration of 15–30 ng μl⁻¹ into embryos, and assayed for rescue. To identify the *foggy* mutation, we used gene-specific primers to amplify genomic DNA from pools of (~5) *foggy* mutant and wild-type sibling embryos. PCR products were directly sequenced using automated cycle sequencers (ABI). cDNAs from mutant and wild-type sibling embryos were synthesized by PCR with reverse transcription (RT-PCR) and sequenced. We used site-directed mutagenesis to introduce the single nucleotide change T to A using reagents from Stratagene.

Transcription assays

A *Nde*I site was created at the 5'-end of the zSpt5 open reading frame by PCR mutagenesis. The *Nde*I (partial)/ *Not*I fragment containing the full-length, wild-type or mutant *foggy* was inserted into *Nde*I–*Bam*HI sites of pET-14b (Novagen), yielding pET-zSpt5 wild-type and pET-zSpt5 mutant. Lysates were prepared from a transformed *Escherichia coli* BL21 (DE3) strain. His₆-zSpt5 proteins were purified from the supernatants by Ni-affinity chromatography, separated by SDS–polyacrylamide gel electrophoresis (SDS–PAGE) and recovered from gel slices. Indicated amounts of recombinant hSpt4 and hSpt5, wild-type or mutant *foggy* were added back to HeLa nuclear extract (2 μl) that was immunodepleted by hSpt4&5 monoclonal antibody. We used pTF3-6C2AT (25 ng) or pSLG402 (125 ng) as a template. To test for stimulatory activity, we used a pSLG402 vector containing a promoter-proximal 85-nucleotide and a promoter-distal 377-nucleotide G-free cassette. The resulting G-free mRNA regions are resistant to RNase T1 digestion, whereas the G-rich linker region is RNase T1 sensitive. After RNase T1 digestion, the two cassettes can be isolated and separated by gel electrophoresis. The molar ratio of the distal cassette, which represents transcription elongation events, to the proximal transcription cassette, which reflects an initiation event, measures the elongation efficiency. The low NTP concentrations were 30 μM ATP, 30 μM GTP, 300 μM CTP and 2.5 μM UTP.

Received 31 May; accepted 17 August 2000.

1. Greenblatt, J. RNA polymerase II holoenzyme and transcriptional regulation. *Curr. Opin. Cell Biol.* **9**, 310–319 (1997).
2. Shilatifard, A., Conaway, J. W. & Conaway, R. C. Mechanism and regulation of transcriptional elongation and termination by RNA polymerase II. *Curr. Opin. Genet. Dev.* **7**, 199–204 (1997).
3. Uptain, S. M., Kane, C. M. & Chamberlain, M. J. Basic mechanisms of transcript elongation and its regulation. *Annu. Rev. Biochem.* **66**, 117–172 (1997).
4. Guo, S. *et al.* Mutations in the zebrafish unmask shared regulatory pathways controlling the development of catecholaminergic neurons. *Dev. Biol.* **208**, 473–487 (1999).
5. Swanson, M. S., Malone, E. A. & Winston, F. SPT5, an essential gene important for normal transcription in *Saccharomyces cerevisiae* encodes an acidic nuclear protein with a carboxy-terminal repeat. *Mol. Cell Biol.* **11**, 3009–3019 (1991).
6. Swanson, M. S. & Winston, F. SPT4, SPT5 and SPT6 interactions: effects on transcription and viability in *Saccharomyces cerevisiae*. *Genetics* **132**, 325–326 (1992).
7. Hartzog, G. A., Wada, T., Handa, H. & Winston, F. Evidence that Spt4, Spt5, and Spt6 control transcription elongation by RNA polymerase II in *Saccharomyces cerevisiae*. *Genes Dev.* **12**, 357–369 (1998).
8. Wada, T., Takagi, T., Yamaguchi, Y., Watanabe, D. & Hande, H. Evidence that P-TEFb alleviates the negative effect of DSIF on RNA polymerase II-dependent transcription *in vitro*. *EMBO J.* **17**, 7395–7403 (1998).
9. Yamaguchi, Y. *et al.* NELF, a multisubunit complex containing RD, cooperates with DSIF to repress RNA polymerase II elongation. *Cell* **97**, 41–51 (1999).
10. Yamaguchi, Y. *et al.* Structure and function of the human transcription elongation factor DSIF. *J. Biol. Chem.* **274**, 8085–8092 (1999).
11. Wada, T. *et al.* DSFI, a novel transcription elongation factor that regulates RNA polymerase II processivity, is composed of human Spt4 and Spt5 homologs. *Genes Dev.* **12**, 343–356 (1998).
12. Yamaguchi, Y., Wada, T. & Handa, H. Interplay between positive and negative elongation factors: drawing a new view of DRB. *Genes Cells* **3**, 9–15 (1998).
13. Cepko, C. L. The roles of intrinsic and extrinsic cues and bHLH genes in the determination of retinal cell fates. *Curr. Opin. Neurobiol.* **9**, 37–46 (1999).
14. Vos, P. *et al.* AFLP: a new technique for DNA fingerprinting. *Nucleic Acids Res.* **23**, 4407–4414 (1995).
15. Higashijima, S., Okamoto, H., Ueno, N., Hotta, Y. & Eguchi, G. High-frequency generation of transgenic zebrafish which reliably express GFP in whole muscles of the whole body by using promoters of zebrafish origin. *Dev. Biol.* **192**, 289–299 (1997).
16. Sullivan, S. L. & Gottesman, M. E. Requirement for *E. coli* NusG protein in factor-dependent transcription termination. *Cell* **68**, 989–994 (1992).
17. Sullivan, S. L., Ward, D. F. & Gottesman, M. E. Effect of *Escherichia coli* nusG function on lambda DNA-mediated transcription antitermination. *J. Bacteriol.* **174**, 1339–1344 (1992).
18. Kyrpides, N. C., Woese, C. R. & Ouzounis, C. A. KOW: a novel motif linking a bacterial transcription factor with ribosomal proteins. *Trends Biochem.* **21**, 425–426 (1996).
19. Hubbard, E. J., Dong, Q., Greenwald, I. Evidence for physical and functional association between EMB-5 and LIN-12 in *Caenorhabditis elegans*. *Science* **273**, 112–115 (1996).

20. Schoenherr, C. J. & Anderson, D. J. The neuron-restrictive silencer factor (NRSF): a coordinate repressor of multiple neuron-specific genes. *Science* **267**, 1360–1363 (1995).
21. Chen, Z. F., Paquette, A. J. & Anderson, D. J. NRSF/REST is required *in vivo* for repression of multiple neuronal target genes during embryogenesis. *Nature Genet.* **20**, 136–142 (1998).
22. Anderson, D. J. & Jan, Y. N. in *Molecular and Cellular Approaches to Neural Development* (ed. Cowan, W. M.) 26–63 (Oxford Univ. Press, New York, 1997).
23. Zorick, T. S., Syrotte, D. E., Brown, A., Gridley, T. & Lemke, G. Krox-20 controls SCIP expression, cell cycle exit and susceptibility to apoptosis in developing myelinating Schwann cells. *Development* **126**, 1397–1406 (1999).
24. Turner, C. A. Jr, Mack, D. H. & Davis, M. M. Blimp-1, a novel zinc finger-containing protein that can drive the maturation of B lymphocytes into immunoglobulin-secreting cells. *Cell* **77**, 297–306 (1994).
25. Persons, D. A. *et al.* Enforced expression of the GATA-2 transcription factor blocks normal hematopoiesis. *Blood* **93**, 488–499 (1999).

Supplementary information is available on Nature's World-Wide Web site (<http://www.nature.com>) or as paper copy from the London editorial office of Nature.

Acknowledgements

We thank E. Chen and P. Ma for help with the AFLP analysis; Y. Yan and J. Postlethwait for anchoring our AFLP markers to the zebrafish genetic map; A. Greenleaf and D. Price for providing the plasmid pSLG402; M. Hynes, J. Lin, B. Lu M. Tessier Lavigne, B. Barres and S. Wilson for critically reading the manuscript; D. Anderson for helpful information; and J. Ligos, A. Bruce and V. Goodwin for help with graphics. Y.Y. is a JSPS Research Fellow. This work was supported in part by a grant-in-aid for Scientific Research on Priority Areas from the Ministry of Education, Sciences, Sports, and Culture of Japan, and a grant from NEDO to H.H.

Correspondence and requests for materials should be addressed to A.R. (e-mail: ar@gene.com). The GenBank accession number for *foggy* is AF288409.

CIC-5 Cl⁻-channel disruption impairs endocytosis in a mouse model for Dent's disease

Nils Piwon*, Willy Günther*, Michael Schwake, Michael R. Bösl & Thomas J. Jentsch

Zentrum für Molekulare Neurobiologie Hamburg, ZMNH, Universität Hamburg, Martinistrasse 85, D-20246 Hamburg, Germany
* These authors contributed equally to this work.

Dent's disease is an X-linked disorder associated with the urinary loss of low-molecular-weight proteins, phosphate and calcium, which often leads to kidney stones^{1,2}. It is caused by mutations³ in CIC-5, a renal chloride channel^{4,5} that is expressed in endosomes of the proximal tubule^{6,7}. Here we show that disruption of the mouse *clcn5* gene causes proteinuria by strongly reducing apical proximal tubular endocytosis. Both receptor-mediated and fluid-phase endocytosis are affected, and the internalization of the apical transporters NaPi-2 and NHE3 is slowed. At steady state, however, both proteins are redistributed from the plasma membrane to intracellular vesicles. This may be caused by an increased stimulation of luminal parathyroid hormone (PTH) receptors owing to the observed decreased tubular endocytosis of PTH. The rise in luminal PTH concentration should also stimulate the hydroxylation of 25(OH) vitamin D₃ to the active hormone. However, this is counteracted by a urinary loss of the precursor 25(OH) vitamin D₃. The balance between these opposing effects, both of which are secondary to the defect in proximal tubular endocytosis, probably determines whether there will be hypercalciuria and kidney stones.

We disrupted the *clcn5* gene by replacing genomic segments encoding the functionally important stretch between transmembrane domains D2 and D5^{8,9} by a lacZ/neomycin cassette (Fig. 1a). This led to a loss of a normal CIC-5 messenger RNA in *clcn5*⁻ mice (Fig. 1b). Western blots using an amino-terminal CIC-5 antibody⁶ indicated that the predicted fusion protein may be unstable (Fig. 1c).

Male *clcn5*^{-/-}, female *clcn5*^{-/-} and female *clcn5*^{+/-} animals grew normally and were fertile. *clcn5*^{-/-} mice did not have kidney stones or nephrocalcinosis even after one year. No changes in kidney morphology and histology were detected. When compared to wild-type (WT) mice, *clcn5*^{-/-} mice produced slightly more urine, which was slightly acidic. *clcn5*^{-/-} mice had no hypercalciuria, but

urinary phosphate excretion was increased by about 50% (see Table in Supplementary Information). *clcn5*^{-/-} mice displayed low-molecular-weight proteinuria. Vitamin D binding protein and retinol binding protein, which is lost into the urine of patients with Dent's disease², were highly elevated in the urine of *clcn5*^{-/-} mice (Fig. S1 in Supplementary Information). Neither proteinuria nor

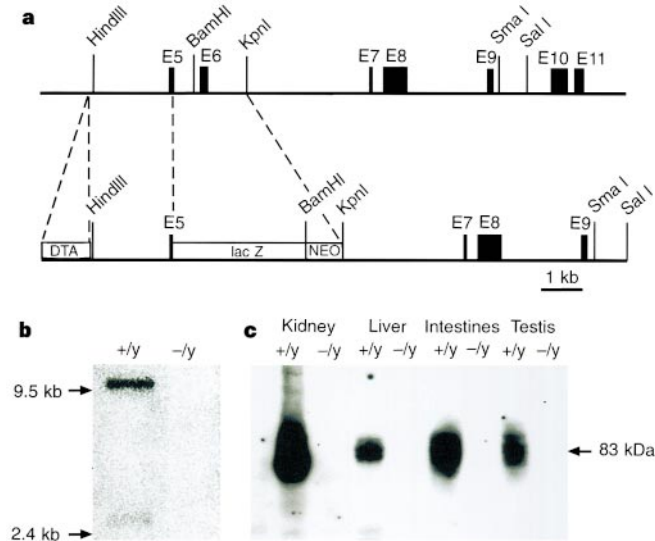


Figure 1 Generation of *clcn5*^{-/-} mice. **a**, Diagram of the targeting vector. Parts of exon 5, exon 6 and the intervening intron are replaced by a lacZ/neo cassette. A diphtheria toxin- α gene (DTA) was fused to select against random integration. **b**, Northern analysis of kidney mRNA from *clcn5*^{+/+} and *clcn5*^{-/-} mice. A probe corresponding to exon 6 detects

CIC-5 mRNA only in WT mice. **c**, Western analysis of membranes from various tissues, using the PEP5A1 N-terminal CIC-5 antibody⁶. Together with immunocytochemical results (Figs 2 and 3), it also confirms the lack of cross-reactivity against the related CIC-3 and CIC-4 proteins.

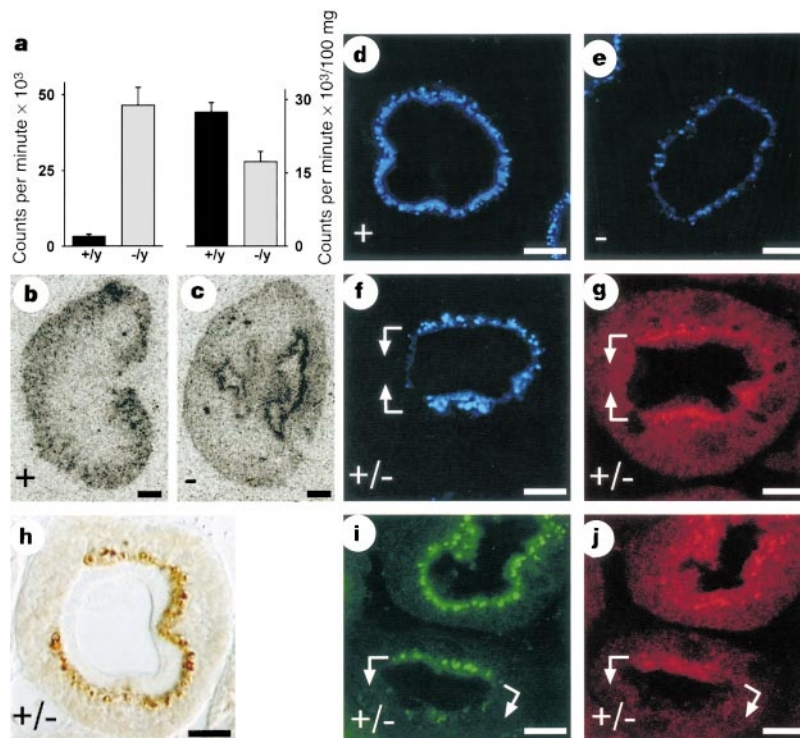


Figure 2 Proximal tubular endocytosis with various *clcn5* genotypes. **a**, ¹²⁵I β_2 -microglobulin excreted into the urine (left) and retained in kidney (right). Autoradiographs of kidney sections of WT (**b**) and *clcn5*^{-/-} (**c**) mice fixed 7 min after injection. **d–f**, Uptake of CY5-labelled β -lactoglobulin (blue; 7-min uptake) into PT cells of *clcn5*^{+/+} (**d**) *clcn5*^{-/-} (**e**), and *clcn5*^{+/-} (**f**) animals. The tubule shown in **f** is stained for CIC-5 (red) in **g**. Cells with reduced endocytosis (between arrows) (**f**) lack CIC-5 (**g**). **h**, Uptake of horseradish

peroxidase (HRP) in a *clcn5*^{+/-} female. Cells with reduced endocytosis probably lack CIC-5, because HRP internalization was drastically lower in *clcn5*^{-/-} mice (data not shown). **i**, Uptake of FITC-dextran (green) in a *clcn5*^{+/-} female. CIC-5 protein in the same tubules is shown in **j**. Bars indicate 10 μ m, except for **b** and **c** (1 mm). Genotypes are indicated in the lower left corner.

phosphaturia were found in a recent mouse model in which the CIC-5 protein, but surprisingly not its mRNA, was moderately reduced using the transgenic expression of a ribozyme¹⁰.

Low-molecular-weight proteins pass the glomerular filter and are normally reabsorbed and degraded by the proximal tubule (PT). By following the fate of labelled proteins that were injected into the bloodstream, we examined whether the proteinuria of *clcn5*⁻ mice is due to defective tubular endocytosis. Iodinated β_2 -microglobulin, a protein whose urinary concentration is drastically increased in Dent's disease^{1,2,11}, was lost into the urine of *clcn5*⁻ mice in much larger quantities than in WT mice (Fig. 2a). This difference in excretion was mirrored by the amount retained within the kidneys. Autoradiography of kidney sections showed that radioactivity had accumulated in the cortex (largely consisting of PTs) of WT kidneys (Fig. 2b), but that it was found in deeper (probably pelvic) regions of *clcn5*⁻ kidneys (Fig. 2c). This indicates a defect in protein uptake by PT cells.

We injected fluorescently labelled lactoglobulin and fixed the kidneys after seven minutes. WT animals had accumulated substantial amounts of the protein in vesicles below the brush border of PT cells (Fig. 2d). By contrast, *clcn5*⁻ tubules had taken up much less protein (Fig. 2e). CIC-5 is encoded on the X-chromosome and is subjected to random X-chromosomal inactivation in females. *clcn5*^{+/-} females are chimaeras, in which cell patches either express or lack CIC-5 protein (Fig. 2g). In chimaeric animals, cells lacking CIC-5 take up much less protein than neighbouring WT cells (Fig. 2f), showing that CIC-5 influences endocytosis in a cell-autonomous manner. CIC-5 disruption also inhibited the endocytosis of horseradish peroxidase (Fig. 2h) and of FITC-dextran, a non-proteinaceous marker for fluid phase endocytosis (Fig. 2i and j). We also determined total uptake of FITC-dextran into WT and *clcn5*⁻ kidneys by measuring the fluorescence of kidney extracts. The elimination of CIC-5 led to a roughly 70% reduction in dextran uptake.

Proximal tubular cells use megalin as an apical receptor to

endocytose a broad range of luminal proteins¹². These include β_2 -microglobulin¹³, vitamin D binding protein¹⁴ and retinol binding protein¹⁵. CIC-5 expression partially overlapped with megalin in the apical pole of PT cells. The amount of megalin was significantly reduced in cells lacking CIC-5 (Fig. 3a–c), which was confirmed by western analysis (Fig. 3i). CIC-5 co-localizes with the proton pump in the subapical region of the PT and in α -intercalated cells of the distal nephron^{6,16}. In contrast to megalin, *clcn5* disruption did not significantly affect the expression of the H⁺-ATPase in either cell type (Fig. S2 in Supplementary Information).

Several transport proteins in the brush border of PTs are regulated by endocytosis. This includes the Na⁺-phosphate cotransporter NaPi-2 (accounting for more than 70% of brush border phosphate transport¹⁷) and the apical Na⁺/H⁺ exchanger NHE3 (involved in reabsorption of Na⁺, HCO₃⁻ and fluid). Both proteins are partially present in endocytotic compartments^{18–20} and are removed from the plasma membrane in response to PTH^{18,21,22}. The NaPi-2 transporter is then degraded in lysosomes. When mice were kept on normal diet, NaPi-2 antibodies²³ stained intensely the brush border of WT PT cells (Fig. 3d). Some subapical vesicles were labelled as well. The staining in *clcn5*⁻ animals was less intense and the protein showed a different subcellular localization (Fig. 3e and f). The brush border was labelled in the early S1 segment (Fig. 3f), but NaPi-2 resided predominantly in subapical vesicles in most other parts of the PT (Fig. 3e). This was unexpected, because a defect in NaPi-2 endocytosis should instead entail an increased presence in the plasma membrane. In chimaeric *clcn5*^{+/-} females, the brush border was stained as intensely as in the WT, irrespective of the expression of CIC-5 (Fig. 3g and h). Thus, the effect of *clcn5* disruption on steady-state NaPi-2 localization is not cell-autonomous. Western analysis confirmed that the amount of NaPi-2 protein was reduced in *clcn5*⁻, but not in *clcn5*^{+/-} animals (Fig. 3i).

These results indicate that a defective regulation of NaPi-2 plasma membrane localization may cause hyperphosphaturia in *clcn5*⁻ mice

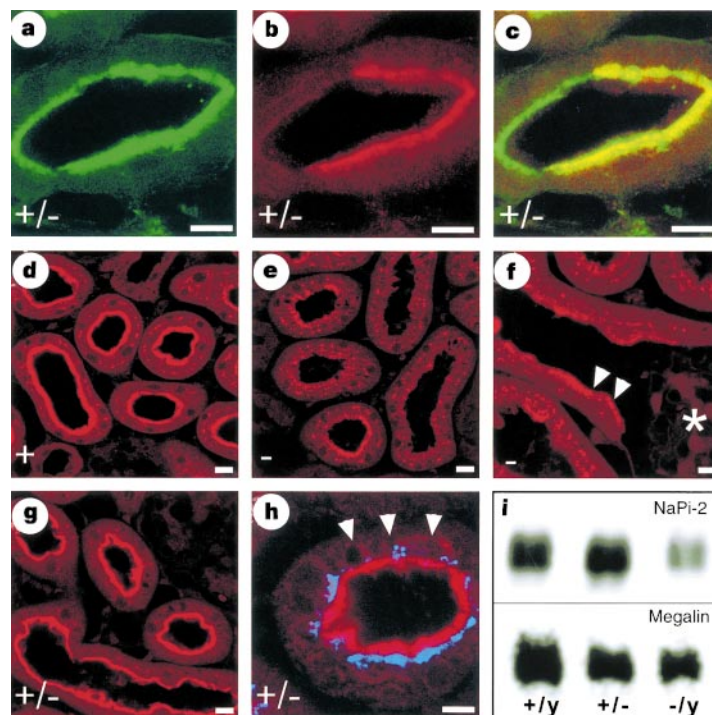


Figure 3 Effect of CIC-5 disruption on transporters and receptors in mice kept on standard diet. A proximal tubule (PT) from a *clcn5*^{+/-} female stained for megalin (green) (a) or for CIC-5 (red) (b). The overlay is shown in c. d–h, NaPi-2 (red) in *clcn5*⁺ (d), *clcn5*⁻ (e, f), and *clcn5*^{+/-} tubules (g, h). In all parts (S1–S3) of the PT of *clcn5*⁺ (d) or *clcn5*^{+/-} (g, h) mice, NaPi-2 shows predominant plasma membrane staining. In h, endocytosed protein (blue) marks CIC-5 expressing cells. Arrows indicate cells with reduced endocytosis. In

clcn5⁻ tubules (e, f), NaPi-2 staining intensity is reduced. NaPi-2 predominantly localizes to vesicles (e) but is also in the plasma membrane of S1 segments (f, arrowheads) close to glomerula (asterisk). i, Western analysis of kidney membranes from *clcn5*⁺, *clcn5*^{+/-} and *clcn5*⁻ animals using antibodies against NaPi-2 (top) and megalin (bottom). Similar results were obtained in four experiments. Bars indicate 10 μ m. Genotype is indicated at lower left.

and in Dent's disease^{1,24}. Depriving mice of dietary P_i enhances plasma membrane expression of NaPi-2 (ref. 18). Also in *clcn5*⁻ mice, this procedure led to a brush-border expression of NaPi-2, which was now similar to the WT (Fig. 4a and b). When P_i-deprived animals were injected with PTH and analysed after 15 minutes, NaPi-2 was internalized in all PT segments of the WT (Fig. 4c and e), but not of *clcn5*⁻ (Fig. 4d and f) animals. Experiments on *clcn5*^{+/-} mice showed that this effect is cell-autonomous (not shown). Thirty minutes after PTH injection, NaPi-2 began to appear in intracellular vesicles of *clcn5*⁻ tubules but was still predominantly apical (Fig. 4f), whereas it was significantly internalized after one hour (Fig. 4g and h).

The slowed, but otherwise apparently intact, regulation of NaPi-2 by PTH, together with the fact that the changed NaPi-2 localization in *clcn5*⁻ mice under standard diet is not cell-autonomous, suggests that altered PTH levels underlie the vesicular localization of NaPi-2 in knockout mice. Serum PTH was only slightly increased in *clcn5*⁻ mice (see table in Supplementary Information). On the other hand, PTH is also present in the glomerular filtrate. PT cells express PTH receptors at both their basolateral and apical membranes²⁵, and apical PTH receptors are functional²⁶. Furthermore, PTH binds to megalin and is endocytosed and degraded in the PT²⁷. This suggests that the defective endocytosis in *clcn5*⁻ mice and the associated downregulation of megalin (Fig. 3a and c) lead to a progressive increase in luminal PTH levels from the early S1 to late S3 segments. The increased stimulation of luminal PTH receptors will enhance the internalization of NaPi-2 (ref. 26). If this hypothesis is correct, NaPi-2 internalization should not be increased in early S1 segments,

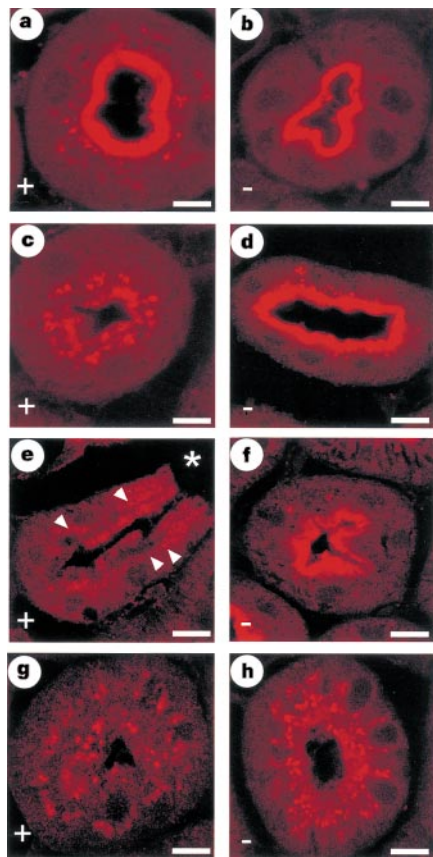


Figure 4 Regulation of NaPi-2 trafficking. **a, b**, NaPi-2 in PTs of phosphate-deprived WT and *clcn5*⁻ mice, respectively. **c–e**, NaPi-2 staining of PTs of phosphate-deprived animals that received PTH for 15 min. **c, e**, *clcn5*⁺; **d**, *clcn5*⁻ mice. **e**, An S1 segment leaving the glomerulus (asterisk). Arrowheads indicate that PTH-induced NaPi-2 internalization occurs also in this segment (a control for the differential localization in *clcn5*⁻ mice on standard diet (Fig. 3e and f)). **f**, NaPi-2 in *clcn5*⁻ mice 30 min after PTH. **g, h**, NaPi-2 1 h after PTH administration to phosphate-deprived *clcn5*⁺ (**g**) or *clcn5*⁻ (**h**) mice. Bars indicate 10 μm.

because PTH levels have not yet risen immediately after filtration. This was indeed observed (Fig. 3f), and contrasts with the uniform internalization of NaPi-2 that is expected for a systemic increase in PTH. This hypothesis additionally predicts an increased urinary loss of PTH. While there is a fourfold increase in urinary PTH in mice lacking megalin²⁷, the less severe defect in megalin-mediated endocytosis in *clcn5*⁻ mice increased urinary PTH by about 1.7-fold (Supplementary Information). Thus, the phosphaturia in *clcn5*⁻ animals may be a consequence of a reduced endocytosis of filtered PTH.

The resulting increase in luminal PTH gives rise to two other predictions. First, the activation of PTH receptors should stimulate the conversion of 25(OH) vitamin D₃ to the active metabolite 1,25(OH)₂-D₃ in the PT. The urinary loss of P_i may also increase 1,25(OH)₂-D₃, as found with the 50% reduction of NaPi-2 gene dosage in *Npt2*^{+/-} mice¹⁷. On the other hand, the reduced endocytosis of vitamin D (VitD) bound to its binding protein leads to a urinary loss of VitD (Supplementary Information) and decreases the availability of the precursor 25(OH) vitamin D₃ within PT cells. Megalin knockout mice, in which receptor-mediated endocytosis of VitD binding protein is totally abolished, display a severe vitamin D deficiency¹⁴. In *clcn5*⁻ mice, serum levels of 25(OH)-D₃ and 1,25(OH)₂-D₃ were reduced about threefold and twofold, respectively (Supplementary Information). Because 1,25(OH)₂-D₃ directly inhibits PTH secretion, this may underlie the slight increase in serum PTH. This contrasts with the slightly elevated levels of 1,25(OH)₂-D₃ and slightly decreased PTH concentrations found in many, but not all, patients with Dent's disease^{1,2,24}. This difference might be explained by a delicate balance between the opposing effects of the increased stimulation of luminal PTH receptors and the decreased availability of 25(OH) VitD₃, both of which result from reduced apical endocytosis. Depending on species, genetic and nutritional factors, this might lead to either an increase or a decrease in 1,25(OH)₂-D₃ concentration. Because 1,25(OH)₂-D₃ stimulates the intestinal absorption of Ca²⁺ and P_i, its increase may result in hypercalciuria and kidney stones in Dent's disease. Because this is an indirect consequence of the defect in endocytosis, the complexity of the interposed hormonal regulation may explain the lack of nephrocalcinosis in our mouse model and the variable clinical picture of *CLCN5* mutations in humans, where proteinuria and phosphaturia are sometimes the only symptoms^{11,24}.

Second, the apical stimulation of PTH receptors should also promote the steady-state internalization of NHE3 in PTs of *clcn5*⁻ mice kept on normal diet. This is indeed true (Fig. 5a and b). Chimaeric females showed that this effect is not cell-autonomous

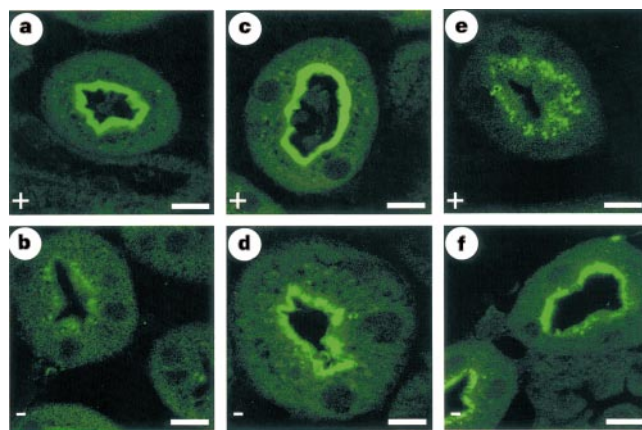


Figure 5 Regulation of NHE3 localization. NHE3 staining (green) of PTs from a WT (**a**) and a *clcn5*⁻ (**b**) mouse kept on standard diet. **c, d**, NHE3 in a phosphate-deprived *clcn5*⁺ (**c**) and *clcn5*⁻ (**d**) mouse. **e, f**, NHE3-stained tubules of a phosphate-deprived WT and *clcn5*⁻ mouse, respectively, 15 min after injection of PTH. Bars indicate 10 μm. Genotype indicated at lower left.

(not shown), and P_i deprivation led to an apical expression of NHE3 also in knockout mice (Fig. 5c and d). PTH stimulation of P_i -deprived mice revealed a slower rate of NHE3 internalization in cells lacking CIC-5 (Fig. 5e and f). This also shows that the proposed endosomal acidification by NHE3 (refs 20 and 28) cannot compensate for the loss of CIC-5. Because NHE3 is an important determinant of salt and fluid transport in the PT^{29} , the decreased surface expression of NHE3 may contribute to the slightly increased urinary volume of CIC-5 knockout mice.

Thus CIC-5 is crucial for efficient endocytosis in the proximal tubule. CIC-5 is the first intracellular chloride channel for which a role in vesicle trafficking is now firmly established. It is very likely that it provides an electrical shunt for the electrogenic proton pump, thereby allowing the efficient luminal acidification that is required for the proper function of the endocytotic pathway⁶. In preliminary experiments, we have indeed found that endosomes purified from *clcn5* kidneys acidify at slower rates than WT endosomes (N.P. *et al.*, unpublished work). However, we cannot exclude that CIC-5 disruption impairs endocytosis by a mechanism that is unrelated to a change in vesicular pH. CIC-5 disruption causes a dramatic slowing, but not complete elimination, of receptor-mediated endocytosis, fluid-phase endocytosis, and the endocytotic retrieval of plasma membrane transporters. On the other hand, it does not play this role in every tissue. We could not detect a significant defect in endocytosis of asialofetuin in the liver (data not shown), an organ that expresses low levels of CIC-5 (ref. 5 and Fig. 1c). This indicates that other chloride channels perform similar roles in other tissues. Our mouse model strongly suggests that alterations in hormones involved in Ca^{2+} homeostasis, and hyperphosphaturia and hypercalciuria, are indirect effects of defective apical endocytosis of PTH and $25(OH)-D_3$; this may explain how a defect in a Cl^- -channel could lead to kidney stones. □

Methods

Generation of *clcn5* mice

Genomic *clcn5* clones were isolated from a mouse λ FixII 129/Sv library (Stratagene) and used to create the targeting vector shown in Fig. 1a. The linearized vector was electroporated into MP12 129/Sv mouse embryonic stem cells. Cells from a correctly targeted clone were injected into C57BL/6J blastocysts that were implanted into foster mothers. Chimaeric males were bred with C57BL/6J females and subsequently crossed into a C57BL/6J background.

In vivo endocytosis and immunocytochemistry

Bovine β -lactoglobulin (Sigma) was labelled with CY5 using a kit (Amersham), and human β_2 -microglobulin (Sigma) with ¹²⁵I using Iodogen (Pierce). Labelled proteins, horseradish peroxidase, or FITC-dextran in PBS were infused into the vena cava of anesthetized mice. At the desired time, the kidneys were fixed by perfusion (through the left heart) with 4% paraformaldehyde or periodate lysine paraformaldehyde in phosphate buffered saline (PBS). Tissue samples were embedded in paraffin, and processed as described⁶. Primary antibodies were the rabbit PEP5A1 anti-CIC-5 antibody⁶, a rabbit antibody against NaPi-2 (ref. 23), the mouse monoclonal 1H2 against megalin³⁰, mouse monoclonals against NHE3 (Chemicon), and monoclonal and polyclonal antibodies against the V-type H^+ -ATPase (gifts from S. Gluck and D. Stone). Horseradish peroxidase was revealed using diaminobenzidine, and primary antibodies were detected with secondary antibodies labelled with Alexa 488 or 546 dyes (Molecular Probes). Sections were examined by laser scanning confocal microscopy (Leica).

Membrane trafficking of NaPi-2

For phosphate depletion, mice were kept on a diet having less than 0.04% phosphate (SSNIF, Soest) for six days. To determine the acute effects of PTH, 20 μ g rat PTH (Bachem) were injected into the vena cava of anesthetized mice together with CY5-labelled lactoglobulin as a control, and kidneys were fixed as described above. For one-hour experiments, mice were first injected intraperitoneally (i.p.) with 80 μ g of PTH, followed after 30 min by an intravenous (i.v.) dose of 20 μ g, and kidneys were fixed after a further 30 min.

Serum and urinary analysis

Blood was drawn from the retro-orbital sinus under light ether anaesthesia. Mice were kept in metabolic cages for urine collection. Creatinine, glucose and salts were determined in the department for clinical chemistry. Serum and urinary PTH, serum $1,25(OH)_2-D_3$, and calcitonin were determined using radioimmunoassays (Immundiagnostik, Nichols Institute Diagnostica and Immutopics). Urinary samples were directly analysed by SDS-polyacrylamide gel electrophoresis (SDS-PAGE), followed by silver staining or western

blotting using polyclonal antibodies against retinol binding protein (from B. Blaner) or vitamin D binding protein (Dako).

Received 29 June; accepted 29 September 2000.

- Wrong, O. M., Norden, A. G. & Feest, T. G. Dent's disease; a familial proximal renal tubular syndrome with low-molecular-weight proteinuria, hypercalciuria, nephrocalcinosis, metabolic bone disease, progressive renal failure and a marked male predominance. *Q. J. Med.* **87**, 473–493 (1994).
- Scheinman, S. J. X-linked hypercalciuric nephrolithiasis: clinical syndromes and chloride channel mutations. *Kidney Int.* **53**, 3–17 (1998).
- Lloyd, S. E. *et al.* A common molecular basis for three inherited kidney stone diseases. *Nature* **379**, 445–449 (1996).
- Fisher, S. E. *et al.* Isolation and partial characterization of a chloride channel gene which is expressed in kidney and is a candidate for Dent's disease (an X-linked hereditary nephrolithiasis). *Hum. Mol. Genet.* **3**, 2053–2059 (1994).
- Steinmeyer, K., Schwappach, B., Bens, M., Vandewalle, A. & Jentsch, T. J. Cloning and functional expression of rat CLC-5, a chloride channel related to kidney disease. *J. Biol. Chem.* **270**, 31172–31177 (1995).
- Günther, W., Lüchow, A., Cluzeaud, F., Vandewalle, A. & Jentsch, T. J. CIC-5, the chloride channel mutated in Dent's disease, colocalizes with the proton pump in endocytotically active kidney cells. *Proc. Natl Acad. Sci. USA* **95**, 8075–8080 (1998).
- Devuyt, O., Christie, P. T., Courtoy, P. J., Beauwens, R. & Thakker, R. V. Intra-renal and subcellular distribution of the human chloride channel, CLC-5, reveals a pathophysiological basis for Dent's disease. *Hum. Mol. Genet.* **8**, 247–257 (1999).
- Jentsch, T. J., Friedrich, T., Schriever, A. & Yamada, H. The CLC chloride channel family. *Pflügers Arch.* **437**, 783–795 (1999).
- Friedrich, T., Breiderhoff, T. & Jentsch, T. J. Mutational analysis demonstrates that CIC-4 and CIC-5 directly mediate plasma membrane currents. *J. Biol. Chem.* **274**, 896–902 (1999).
- Luyckx, V. A., Ledercq, B., Dowland, L. K. & Yu, A. S. Diet-dependent hypercalciuria in transgenic mice with reduced CLC5 chloride channel expression. *Proc. Natl Acad. Sci. USA* **96**, 12174–12179 (1999).
- Morimoto, T. *et al.* Mutations in CLCN5 chloride channel in Japanese patients with low molecular weight proteinuria. *J. Am. Soc. Nephrol.* **9**, 811–818 (1998).
- Lehese, J. R. *et al.* Megalin knockout mice as an animal model of low molecular weight proteinuria. *Am. J. Pathol.* **155**, 1361–1370 (1999).
- Orlando, R. A. *et al.* Megalin is an endocytic receptor for insulin. *J. Am. Soc. Nephrol.* **9**, 1759–1766 (1998).
- Nykjaer, A. *et al.* An endocytic pathway essential for renal uptake and activation of the steroid 25-(OH) vitamin D₃. *Cell* **96**, 507–515 (1999).
- Christensen, E. I. *et al.* Evidence for an essential role of megalin in transepithelial transport of retinol. *J. Am. Soc. Nephrol.* **10**, 685–695 (1999).
- Sakamoto, H. *et al.* Cellular and subcellular immunolocalization of CIC-5 channel in mouse kidney: colocalization with H^+ -ATPase. *Am. J. Physiol.* **277**, F957–F965 (1999).
- Beck, L. *et al.* Targeted inactivation of Npt2 in mice leads to severe renal phosphate wasting, hypercalciuria, and skeletal abnormalities. *Proc. Natl Acad. Sci. USA* **95**, 5372–5377 (1998).
- Murer, H. *et al.* Posttranscriptional regulation of the proximal tubule NaPi-II transporter in response to PTH and dietary Pi. *Am. J. Physiol.* **277**, F676–F684 (1999).
- Biemesderfer, D. *et al.* Monoclonal antibodies for high-resolution localization of NHE3 in adult and neonatal rat kidney. *Am. J. Physiol.* **273**, F289–F299 (1997).
- D'Souza, S. *et al.* The epithelial sodium-hydrogen antiporter Na^+/H^+ exchanger 3 accumulates and is functional in recycling endosomes. *J. Biol. Chem.* **273**, 2035–2043 (1998).
- Traebert, M., Roth, J., Biber, J., Murer, H. & Kaissling, B. Internalization of proximal tubular type II Na-Pi cotransporter by PTH: immunogold electron microscopy. *Am. J. Physiol.* **278**, F148–F154 (2000).
- Zhang, Y. *et al.* In vivo PTH provokes apical NHE3 and NaPi2 redistribution and Na-K-ATPase inhibition. *Am. J. Physiol.* **276**, F711–F719 (1999).
- Custer, M., Lotscher, M., Biber, J., Murer, H. & Kaissling, B. Expression of Na-Pi cotransport in rat kidney: localization by RT-PCR and immunohistochemistry. *Am. J. Physiol.* **266**, F767–F774 (1994).
- Bosio, M., Bianchi, M. L., Lloyd, S. E. & Thakker, R. V. A familial syndrome due to Arg648Stop mutation in the X-linked renal chloride channel gene. *Pediatr. Nephrol.* **13**, 278–283 (1999).
- Kaufmann, M. *et al.* Apical and basolateral parathyroid hormone receptors in rat renal cortical membranes. *Endocrinology* **134**, 1173–1178 (1994).
- Traebert, M., Völk, H., Biber, J., Murer, H. & Kaissling, B. Luminal and contraluminal action of 1-34 and 3-34 PTH peptides on renal type IIa Na-Pi cotransporter. *Am. J. Physiol.* **278**, F792–F798 (2000).
- Hilpert, J. *et al.* Megalin antagonizes activation of the parathyroid hormone receptor. *J. Biol. Chem.* **274**, 5620–5625 (1999).
- Gekle, M. *et al.* Inhibition of Na^+-H^+ exchange impairs receptor-mediated albumin endocytosis in renal proximal tubule-derived epithelial cells from opossum. *J. Physiol. (Lond.)* **520**, 709–721 (1999).
- Schultheis, P. J. *et al.* Renal and intestinal absorptive defects in mice lacking the NHE3 Na^+/H^+ exchanger. *Nature Genet.* **19**, 282–285 (1998).
- Zheng, G. *et al.* Organ distribution in rats of two members of the low-density lipoprotein receptor gene family, gp330 and LRP/alpha 2MR, and the receptor-associated protein (RAP). *J. Histochem. Cytochem.* **42**, 531–542 (1994).

Supplementary information is available on Nature's World-Wide Web site (<http://www.nature.com>) or as paper copy from the London editorial office of Nature.

Acknowledgements

We thank G. Boia for technical assistance, P. Gruss for MPI2 ES cells, H. Murer and J. Biber for the NaPi-2 antibody, R. McCluskey for the megalin antibody, S. Gluck and D. K. Stone for proton pump antibodies, B. Blaner for the antibody against retinol binding protein and M. Haddad for chemical analysis of serum and urine samples. This work was supported by grants from the Deutsche Forschungsgemeinschaft, the Fonds der Chemischen Industrie, and the Louis-Jeantet Prize for medicine to T.J.J.

Correspondence and requests for materials should be addressed to T.J.J. (e-mail: jentsch@plexus.uke.uni-hamburg.de).